Optimisation of Debinding Using Experiment-Based Computational Concepts

G. Seifert, H. Ziebold, F. Raether

Debinding causes quality problems with manufacturing of many ceramic components. A systematic approach is presented to solve debinding problems using a careful analysis of the initial situation, a customised measuring concept and experiment-based simulations. User apps are developed which enable the operator to optimise debinding cycles for various component shapes.

1 Introduction

The manufacturing of high-quality ceramic parts, e.g., with six sigma tolerances requires the reliable control of the debinding process. Organic additives like binders, plasticisers or dispersants, necessary to enable smooth forming of green parts, have to be removed before the parts can be heated to sintering temperatures. Besides few special cases, where chemical debinding methods are applied, the vast majority of ceramic green parts is prepared for sintering by thermal debinding processes. With thermal debinding, the organic additives, in summary denoted as binder, are converted into gaseous reaction products by combustion or pyrolysis reactions. The gases first have to permeate the porous green body, before they are transported to the exhaust gas system of the furnace and finally are completely mineralized to CO_2, H_2O etc. in an afterburning system.

A number of problems can occur during debinding (Fig. 1). Temperature and pressure gradients within the green part cause stresses, which are increasingly critical when the compact becomes more and more fragile during binder removal. If local stresses exceed the temporary strength of the compacts, cracks are formed or parts decompose (Fig. 1 a–b); laminated green parts can delaminate (Fig. 1 c).

Uneven distribution of organic molecules during debinding can cause gradients in the elemental concentration after debinding (Fig. 1 d). E.g., residual carbon may be concentrated in the interior of the part or oxides of polyvalent metals are reduced. If thermoplastic binders are used their liquefaction during heating can cause warping of the compacts, if stresses occur (Fig. 1 e). Such stresses can arise from the aforementioned pressure and temperature gradients but as well from uneven binder distribution, gravity and friction. Binder liquefaction can also effect microstructure homogeneity. Capillary forces lead to a local redistribution of binder and particle rearrangement. If gaseous pyrolysis products form in regions with high binder concentration, large bubbles arise (Fig. 1 f). Regions with high particle concentration, formed by the capillary forces, tend to preferred sintering and grain growth during the subsequent heat treatment.

All six phenomena shown in Fig. 1 a–f deteriorate the quality of the sintered ceramic parts or enhance the scrap rate. Moreover, an inflammation of carbonization gases from the debinding process may occur, if their concentration in the furnace reaches a critical level. This often induces total loss of the charge and damage at the furnace. In addition, carbonization gases may be transferred to colder parts within the furnace, where they condense and contribute to special debinding issues. To overcome all these problems a sophisticated strategy is required, which is tailor-made to the specific debinding process. Such a strategy has

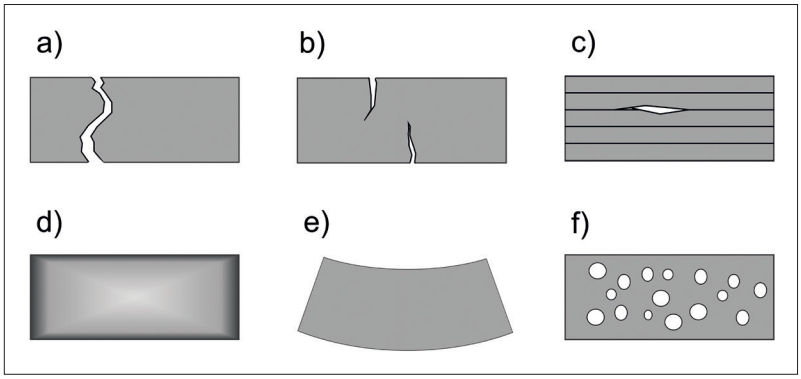

Fig. 1 a–f Schematic sketches of six typical cases of damage of ceramic components which can occur due to insufficient debinding: a) fracture, b) crack formation, c) delamination, d) gradient formation, e) warpage, f) formation of large pores

G. Seifert, H. Ziebold, F. Raether
Fraunhofer Institute for Silicate Research, Center for High Temperature Materials and Design HTL
95448 Bayreuth, Germany

Corresponding author: G. Seifert
E-mail: gerhard.seifert@isc.fraunhofer.de

Keywords: debinding, Finite Element Model (FEM), thermal process optimisation

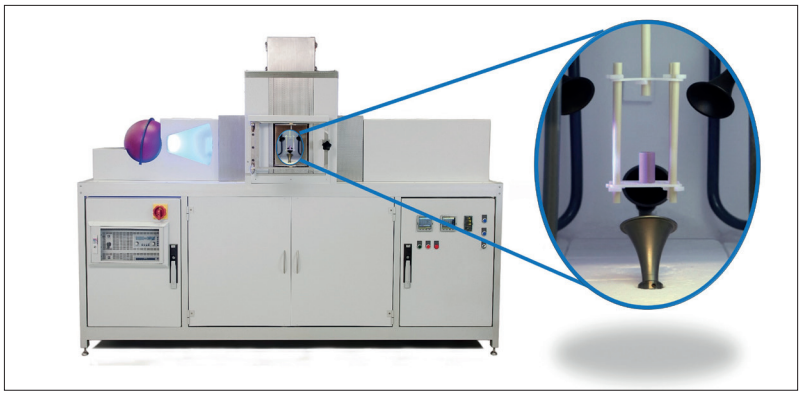

Fig. 2 Thermooptical Measuring Device TOM_air for investigations of debinding by simultaneous weight measurement, optical dilatometry and sound emission analysis

been developed at Fraunhofer Center HTL. It is based on the triple jump: Analyse, Measure, Improve (AMI) and will be outlined in the subsequent chapter

2 The AMI strategy for thermal debinding processes

In the first step, the debinding problem is carefully analysed using the existing knowledge base about the process. Starting from the phenomena leading to debinding problems, a decision tree is used to obtain exactly those data which are required to plan the next step. These data can include information about the green compacts, the furnace or the process.

Important parameters of the green compact are binder volume fraction (can be estimated for the forming process used), component dimensions (especially wall thickness) and shape. Knowledge of the binder type, in particular its possible thermoplastic behaviour, is helpful. Moreover, green density and particle size are useful to estimate gas permeation. Not least, possible quality problems already existing in the green compact are to be discussed, because they rarely can be eliminated during the heat treatment [1].

Relevant information on the applied furnace can be its type, heating method (gas fired or resistance heated), heat transfer to the charge (radiation, convection, ventilated gas circulation), useful volume, filling level and temperature distribution. For the thermal process, arrangement of components, furnace atmosphere, gas flow and heating rates are important. Also drying steps possibly required to remove residual solvents may be an issue.

Based on this information, a measuring concept for the investigation of debinding phenomena is designed. Various measuring methods are available, which can be arranged in four groups:

1 In situ measurements, which are performed in lab furnaces during debinding of green samples. At the center HTL, different Thermooptical Measuring Devices (TOM) were developed (Fig. 2). They can reproduce the atmosphere of the industrial process and provide all relevant data for inspection of the debinding process [2].
2 High temperature material characterisations, which are required to obtain auxiliary data for computer simulation of the debinding process. Mostly methods of thermal analysis can be used for this purpose, which are commercially available [2].
3 Characterisations of industrial furnaces, which deliver special data, e.g. on gas flow within the furnace. A mobile test rig has been developed for these characterisations at Fraunhofer Center HTL, which can be used to measure missing data of the furnace [3].
4 Chemical and structural analysis of green or partially debinded samples at ambient temperature.

In order to minimise experimental effort, only those methods relevant for problem solving are selected. The measuring concept may continue the decision tree to obtain missing information successively. E.g., if the debinding problems suggest a liquefaction of the binder, but the binder is unknown, the debinding process can be performed in a TOM-furnace where shape changes are detected in situ (compare Fig. 2). The local binder distribution is analysed in partially debinded and quenched samples using a special sample preparation by Cross Section Polishing (CSP) and Scanning Electron Microscopy (SEM) [4]. Another example is a possible redistribution of carbonization gases by evaporation from hotter green parts and condensation at cooler green parts within the furnace. In that case, the mobile test rig for furnace measurement can be used to obtain missing information.

In the third step, the debinding process is improved. Usually a combination of computer simulation and experimental validation is used in this step. Problem solving aims at measures which can be implemented with minimal modification of current production. Considering the first example above, problems with liquefaction of the binder are therefore preferentially solved without exchanging the binder. Instead, the period with liquid binder is minimised and a thermal crosslinking of binder molecules in a lower temperature stage may be introduced [4]. In the second example, the minimal process change may be the change of the gas flow in the furnace.

The principles of the AMI approach are summarised in Fig. 3. The presentation of all possible routes would by far go beyond the scope of the current article. Since the damage related to internal stresses occurs most frequently, the AMI approach is exemplified in this context in the next chapter.

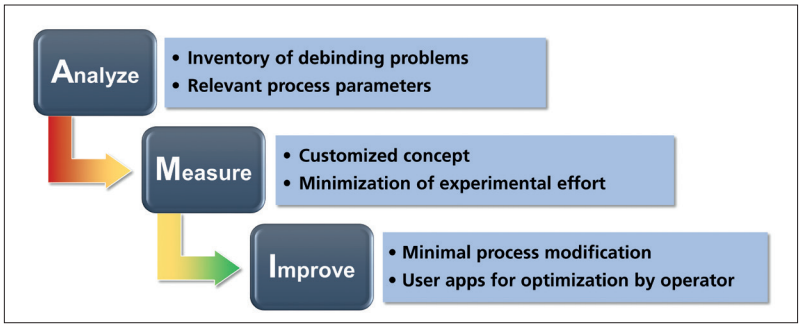

Fig. 3 Principles of the AMI approach

3 Avoiding critical stresses during debinding

When internal stresses during debinding exceed the actual strength of the compact, cracking, fracture or delamination may occur. There are two sources of such stresses:

A) transport of gaseous products of binder decomposition within the green parts can lead to local overpressure;
B) temperature gradients due to limited heat flow during heating of the green parts, usually enhanced by exo- and endothermic debinding reactions.

A still widespread approach to remain on the safe side is to deploy very slow heating rates, leading to extremely long-lasting debinding cycles of several days. While this practice avoids costly scrap rates on the one hand, it is on the other hand economically critical because of high energy consumption and low throughput of the furnace. This, in turn, creates a strong need for debinding conditions, which provide the fastest temperature cycle, which is still safe with respect to component damage. In principle, the key processes controlling polymer decomposition and mass and heat transport have been well understood for a long time [5, 6]. However, the complexity of chemical reactions and the large number of parameters in industrial debinding processes make it difficult to consider these effects explicitly in practical debinding optimisation.

In the analysis step of the AMI approach for stress reduced debinding, some issues are important: pressure gradients increase with increasing binder volume fraction, since permeability decreases and pressure compensation by gas flow is reduced. The binder volume fraction depends on the forming method – increasing from dry pressing over slip casting, tape casting, extrusion to injection moulding. Gas and heat transfer also depend on the wall thickness of the compact – making it more difficult to optimise debinding of large components. As a rule of thumb, above typical sample dimensions of $L \approx 1$ cm an explicitly spatially resolved model is required to find an optimal temperature cycle for debinding [7]. If high heating rates or binder volume fractions are to be considered, spatially resolved models have to be used already at smaller wall thickness.

The measuring concepts developed at Fraunhofer Center HTL depend mainly on binder volume fraction, wall thickness and previous knowledge on the process. Measuring methods, their acronyms and several concepts are summarised in Tab. 1. A higher concept number includes all measurements required for lower concept numbers. This means that TG measurements are always required. Weight loss provides an accurate measure for the degree of reaction during debinding. It is measured using very small samples representing a small volume in the real green compact. MS measurements do not require additional runs (compare Tab. 1), because they are performed simultaneously to TG using a combined TG-DSC-MS device. Most tedious is the mechanical testing, since the partially debinded samples are extremely fragile. The range shown in the column for the number of runs in Tab. 1 essentially depends on the envisaged level of accuracy. The numbers in the category column refer to the four groups of measuring methods outlined in Chapter 2, the letters A and B to the two sources of stresses defined above.

Tab. 1 **Measuring methods required for the various concepts of the AMI approach to eliminate stress induced damage during debinding (explanations of columns are given in the text)**

Method	Acronym	Property	Category	Concept	# Runs
Thermogravimetry	TG	Sample weight	1A, 1B	1	3–10
Sound emission	SEA	Crack detection	1A, 1B	1	1–6
Differential scanning calorimetry	DSC	Heat of reaction	1B	2	2
Laser-flash	LFA	Thermal diffusivity	1B	2	1
Mass spectrometry	MS	Mass number of gas species	1A	3	0
Carrier gas hot extraction	CGHE	Total formula of binder	4A	3	2
Gas flow measurement	GFM	Permeability	4A	3	3–5
4-point bending	FPBT	Strength, Young's modulus	2A, 2B	4	5–10

The measured data have to be parametrised to obtain smooth functions, which can be used in debinding simulations. For that, an important reduction of complexity is obtained by separating temperature effects and the degree of debinding using the well-known principle of additivity:

$$P(S, T) = P'(S) \cdot P''(T) \qquad \text{(eq. 1)}$$

P, P′ and *P″* denote parametric functions for any of the parameters. The variables *S* and *T* are degree of debinding and temperature, respectively. The degree of debinding itself is obtained from TG measurements at different heating rates using the so-called kinetic field method. It was shown by the authors that this method is very robust and enables an accurate prediction of debinding rates [8, 9].

Concept 1 can be used for debinding optimisation of small compacts. Only 3–5 TG measurements are required to set up the kinetic field. Based on the kinetic field, several time-temperature cycles with constant debinding rate are calculated. These cycles are tested in a TOM device equipped with microphones for SEA. It was shown previously that SEA is very sensitive for crack detection during debinding [10]. A special design of the SEA using several microphones has been developed to obtain an excellent filtering of real signals from noise signals [11]. The fastest heating cycle without crack signals is selected as the optimum.

Concept 2 can be applied to large compacts with low or moderate binder volume fractions, if some information is already available on acceptable debinding conditions. If the industrial debinding is performed in inert gas, 3–5 TG measurements in inert gas atmosphere are sufficient for the construction of the kinetic field. If industrial debinding is performed in oxidic atmosphere, an additional kinetic field measured in oxidic atmosphere is required. Additionally, thermal diffusivity is measured with and without binder, which can be done in one temperature cycle during heating and cooling of a green sample. Simulations are done in a thermal Finite Element (FE) model

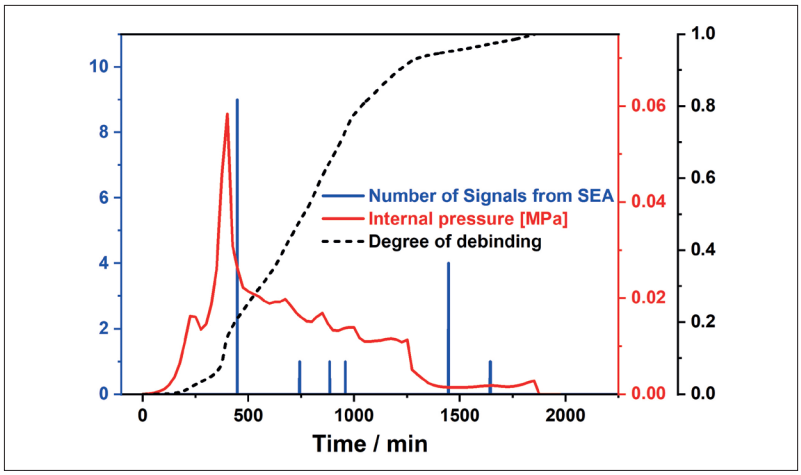

Fig. 4 Comparison of measured degree of debinding, calculated internal pressure and Acoustic Detections (SEA) for a 3D-printed alumina sample

where the component is heated in small steps and the local debinding rates are calculated considering local temperature and local degree of debinding. If debinding is performed in oxidic atmosphere at the outside of the component, the respective kinetic field is applied with exothermic heat of reaction. In interior regions of the component, the kinetic field obtained in inert gas atmosphere with endothermic heat of reaction is used, because the outward flow of pyrolysis gases hinders oxygen diffusion into the reaction zone. Heat flow is calculated based on measured thermal diffusivity data using an interpolation according to local degree of debinding. Optimisation is done starting from known debinding cycles and varying heating conditions in order to minimise thermal stresses and debinding time.

Concept 3 has been developed for debinding of large components with high binder volume fractions. As for Concept 2, information on acceptable debinding conditions is required. In addition to Concept 2, gas flow is explicitly included in the model and the overpressure is calculated. Permeability of partially debinded samples is determined at room temperature by gas flow measurements and extrapolated to higher temperatures using gas theory [12]. The FE model considers permeation and interdiffusion of the gas species within the pore channels. It assumes complete mineralization of pyrolysis gases if enough oxygen is available. The mass number of the pyrolysis gas is obtained from MS measurement. Reaction products during mineralization are balanced according to the total formula of the binder measured by CHGE. Optimisation is done starting from known debinding cycles and varying heating conditions in order to minimise thermal stresses, overpressure and debinding time.

The interplay of experiment and simulation creates important insights into the debinding behaviour. This is illustrated by Fig. 4, which refers to debinding of an alumina green sample with high binder volume fraction manufactured by stereo lithography. In Fig. 4, as a function of time, the measured average degree of debinding is plotted together with the calculated internal overpressure and the experimentally observed acoustic emissions. Clearly the strongest acoustic signals are correlated with the peak of internal pressure, indicating most probably cracks occurring within the sample.

Concept 4 can be used for all types of green compacts without previous knowledge on the debinding process. However, as with the other three concepts, it has to be excluded that liquefaction phenomena play an adverse role during debinding. In addition to Concept 3, also the mechanical

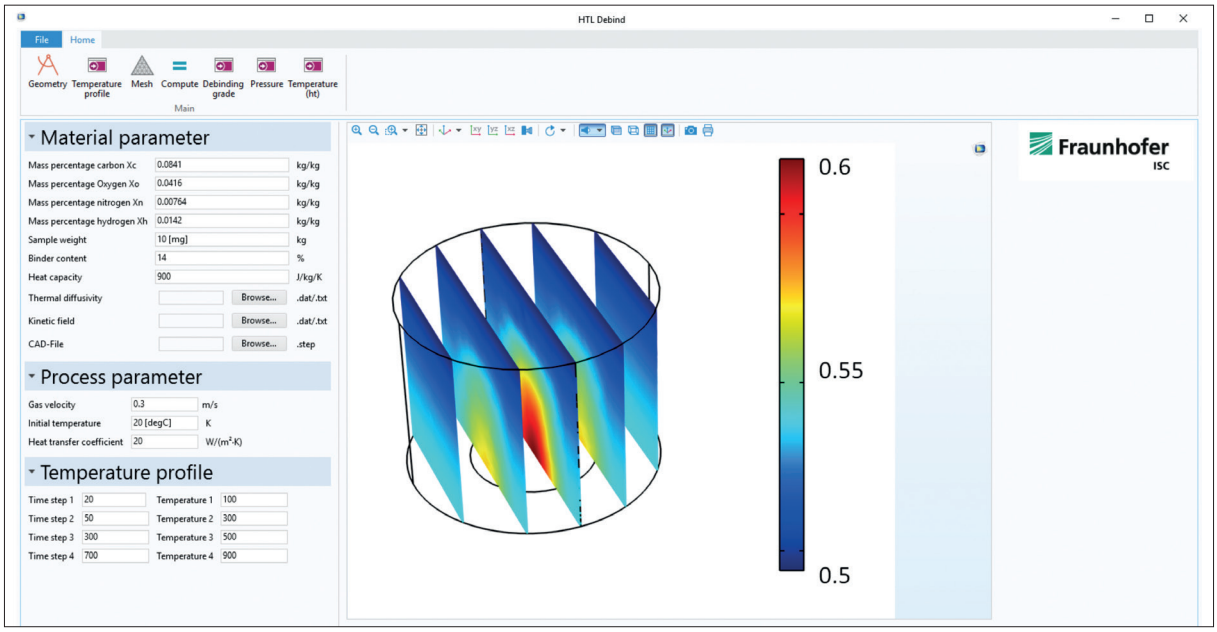

Fig. 5 Example for the GUI of a debinding app

properties of partially debinded samples have to be measured. For that, always eight green samples are mounted in a multiple sample holder – specially constructed for FPBT – and partially debinded at different temperatures. Thereafter, the samples are heated to the measuring temperature, which is well below the debinding temperature, and successively broken by a push rod in one heating run. From the stress-strain curves, Young's modulus and bending strength are derived. In addition, thermal expansion is required, which can be measured using dilatometry. Putting all these parametrised data together, a coupled thermal, kinetic, mass-flow and mechanical FE analysis is performed in small temperature steps.

Optimisation of debinding conditions is done by minimising debinding time regarding all internal stresses, which have to remain well below the fracture strength.

Before the optimised debinding conditions are transferred to industrial furnaces, it is beneficial to validate the simulation in a measuring furnace.

Various lab furnaces for measuring weight loss during debinding in different atmospheres are available at the Fraunhofer Center HTL for this purpose – some being equipped with additional SEA [2].

An example for validation of debinding simulation on a large sample (refractory brick) according to Concept 3 was already published [13].

4 Development of user apps for stress reduced debinding processes

Currently, the model which has been applied successfully to several industrial cases in the last years is being further developed to yield independently functional software packages (apps) enabling industrial users to perform systematic, component-specific debinding optimisation on their own. The models for Concepts 1, 2, 3 or 4 respectively, and the respective parametrised experimental data described in the previous section are implemented in the corresponding apps. The user can vary the component shape using a standard interface for the input of geometry data (e.g., in the STL format), and can find the optimum temperature cycle by his own priorities. Fig. 5 shows the Graphical User Interface (GUI) of a debinding app. The coloured 3D-representation in the Fraunhofer Center of the screenshot in Fig. 5 shows the spatial distribution of the degree of debinding at an intermediate stage obtained from the simulation.

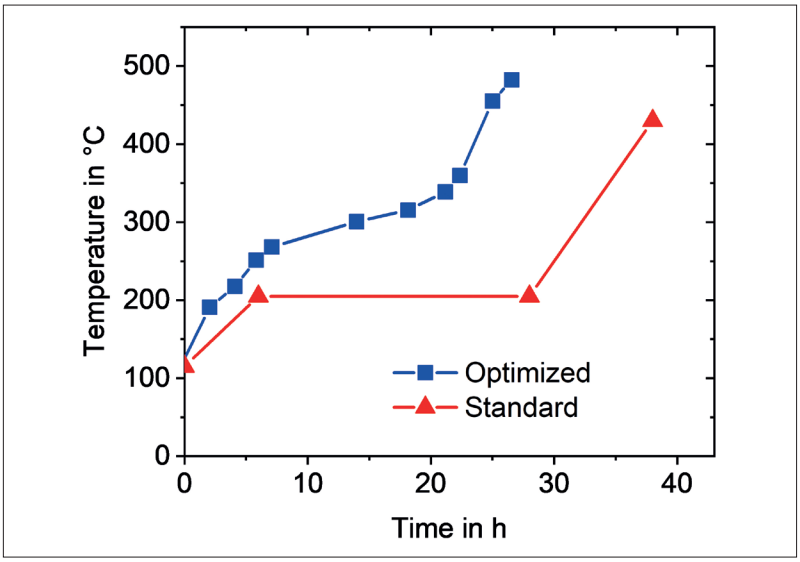

Fig. 6 Comparison of standard temperature profile for debinding with profile optimised by Concept 1

Fig. 6 shows an example for the optimisation of a temperature profile using Concept 1. For that, alumina green parts printed by stereo-lithography were selected. Wall thickness was 1 cm. The optimised temperature profile is considerably shorter than the standard profile previously used. Likewise, it avoided cracking during debinding, which had been a problem using the standard profile.

Acknowledgements

The authors gratefully acknowledge the help of M. Stepanyan, J. Baber, T. Martini, M. Roth, H. Zorzytzki, H. Friedrich and W. Bernstein with the measurements as well as financial support of the Federal State of Bavaria within the project DiMaWert.

References

[1] Raether, F.: Energy efficiency during production of ceramics. cfi/Ber. DKG **90** (2013) [10] E1–E4

[2] www.htl.fraunhofer.de/en/FocusOfResearch/characterization/thermooptical_measuring_devices_tom.html, visited 2021/03/29

[3] www.htl.fraunhofer.de/en/FocusOfResearch/manufacturing_processes/furnace_technology/industrial_furnace_analysis.html, visited 2021/03/29

[4] Brunner, D.G.; Raether, F.; Klimera, A.: Debindering of non-oxide ceramics under protective atmosphere. Ceramic Transactions **215** (2009) 77–86

[5] Lewis, J.A.: Binder removal from ceramics. Ann. Rev. Mater. Sci. **27** (1997) 147–173

[6] German, R.M.: Theory of thermal debinding. Int. J. Powder Metall. **23** (1987) 237–245

[7] West, A.C.; Lombardo, S.J.: The role of thermal and transport properties on the binder burnout of injection-molded ceramic components. Chem. Engin. J. **71** (1998) 243–252

[8] Raether, F., Klimera, A.: Methods of measurement and strategies for binder removal in ceramics. In: Herrmann, M.; Clasen R. (eds.): Thermal process engineering in the ceramics industry. Göller Verlag, Baden-Baden 2008, 5–11

[9] Raether, F.: The kinetic field – a versatile tool for prediction and analysis of heating processes. High Temperature – High Pressures **42.4** (2013) 303–319

[10] Raether, F. (ed.): Nachhaltige Wärmebehandlungsprozesse systematisch entwickeln. Frankfurt 2018

[11] Raether, F.; Schmidt, I.: Modellierung und Simulation. In: Raether, F. (ed.): Energieeffizienz bei der Keramikherstellung, Frankfurt 2013, 74–96

[12] VDI Wärmeatlas – Berechnungsblätter für den Wärmeübergang: Ed. Verein Deutscher Ingenieure, VDI-Gesellschaft Verfahrenstechnik und Chemieingenieurswesen, Berlin Heidelberg, New York 2002

[13] Ziebold, H.; Raether, F.; Seifert, G.: Radical time reduction of debinding processes by combined in situ measurements and simulation. cfi/Ber. DKG **95** (2018) [1–2] E 37–E 40